CETRA2024 15-17 May 2024, Cavtat, Croatia
8th International Conferenceon Road and Rail Infrastructure

WIND TUNNEL TESTING OF A CABLE STAYED BRIDGE PYLON

Roberto Gomez, Marco Antonio Mendoza, Raul Sanchez, Oscar Rosales
Institute of Engineering, UNAM, Mexico

Abstract

One of the objectives of wind tunnel aeroelastic testing for bridges in smooth or very turbulent flows is to identify the potential of vortex-detached vibration and verify that wind speeds associated with the flutter instability are sufficiently high. This document shows the experimental methodology used for the study of the aeroelastic behaviour of a pylon of a cable-stayed bridge, which will be located in México City. Measurements of the response of the pylon were performed at four different wind azimuths in relation to the longitudinal axis of the bridge; i.e. 0° (along the axis of the bridge), 30°, 60°, and 90° (perpendicular to the axis of the bridge), taking advantage of the symmetry of the bridge for these measurements. The results of the analysis are presented in terms of forces, moments and displacements in different sections of the model; low turbulence and turbulent wind flows that reproduce the local conditions at the site were simulated in an atmospheric boundary layer wind tunnel. Construction and service stages of the bridge are considered. Based on the analysis of the results, final comments and recommendations are issued.

Keywords: wind tunnel testing, vortex shedding, flutter, bridge aeroelastic models, structural dynamic response

1 Introduction

The purpose of wind tunnel testing under smooth or very turbulent flows is to identify the rise of vortex-detached vibration and verify that wind speeds associated with flutter instability are sufficiently high [1]. In a first stage of work, measurements of the response of pylon 3 of a cable-stayed bridge were performed at four different wind azimuths in relation to the longitudinal axis of the bridge; i.e. 0° (along the axis of the bridge), 30°, 60°, and 90° (perpendicular to the axis of the bridge) and taking advantage of the symmetry of the tower for these measurements. Angles of 90, 120°, 150° and 180° were revised for the pylon and deck model. The main towers are important components of long-span suspension and cable-stayed bridges. However, a freestanding bridge tower in its construction state is generally characterized with low structural damping and lower natural vibration frequencies than when the bridge deck and cables are attached and the structure is totally isolated. In this case, the tower is more vulnerable to across-wind dynamic responses associated with wind–structure interactions [2].
Based on the information provided by the owner, the wind criteria for the design of the bridge required that the completed bridge do not show any instability up to a mean hourly wind speed of 36 m/s, corresponding to a 200 years of return period. In addition, the bridge was studied with a mean hourly wind speed of 29 m/s with a 10 years of return period for the construction stage.

DOI: https://doi.org/10.5592/CO/CETRA.2024.1698

In this paper, in the first stage, we present the preliminary results obtained from the testing of an aeroelastic model of an isolated pylon at bridge scale. Smooth and turbulent flow was simulated in the wind tunnel. Based on the observed behaviour, a more complete model, which included part of the superstructure, was designed and fabricated; this model was used to simulate a double cantilever construction stage of the bridge and to verify the behaviour of the bridge to aerodynamic instabilities.

2 Aeroelastic model of the bridge

2.1 Similitude law criteria

The geometric scale was 1:200. The resulting (Froude scaled) velocity ratio is 14.14:1 between the prototype and the model. Based on the prototype structure and the overall principles of aeroelastic model design [3] the pylon and deck model were composed of an aluminium core beam (simulating the stiffness), Polylactic acid (PLA) coats (simulating the shape of the deck) and brass compensating weights. The compensating weights were installed in the PLA coats to adjust the mass and mass moment of inertia of the pylon and the deck of the bridge. The cables in the model were made of inextensible nylon wires, but to simulate equivalent axial stiffness, each cable was provided by an extension spring situated at deck level. The cables were wrapped with polyethylene tubing, which allowed us to model the drag forces on the cables appropriately.

2.2 Instrumentation

A Wheatstone half-bridge array with active gauges was used at each location where bending stresses were measured at the isolated pylon model [4]. A six-degree-of-freedom load cell at the base was also incorporated to measure forces and moments [5]. Figure 1 shows the locations to measure flexural strains generated by wind pressure in the longitudinal direction (S9, S10, S11, S12), and in the transverse direction (S13 and S14).
Regarding the pylon and deck model, Figure 2 shows the location of the sensors at the deck. Arrays of sensors (S15 and S16) were tested in a Wheatstone full-bridge configuration which improved the stability of measurements [4]. In addition, an inclinometer which incorporates a triaxial accelerometer and a MEMS gyroscope (S5) [6] was used, as well. Four distance laser sensors (S1, S2, S3, and S4) were installed at the sections A and B [7].

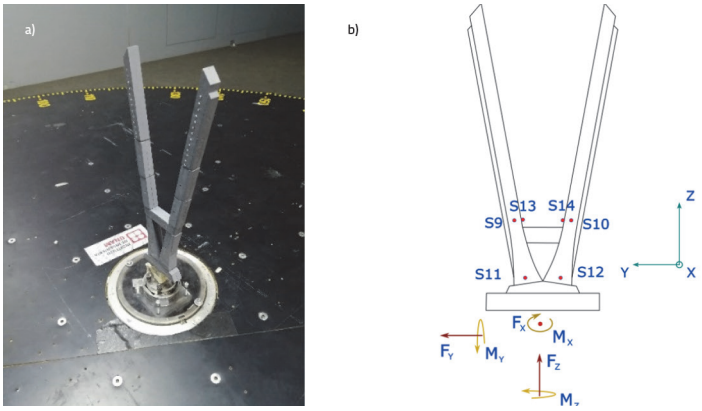

Figure 1 a). Isolated pylon model; b). Sign convention and sensors location

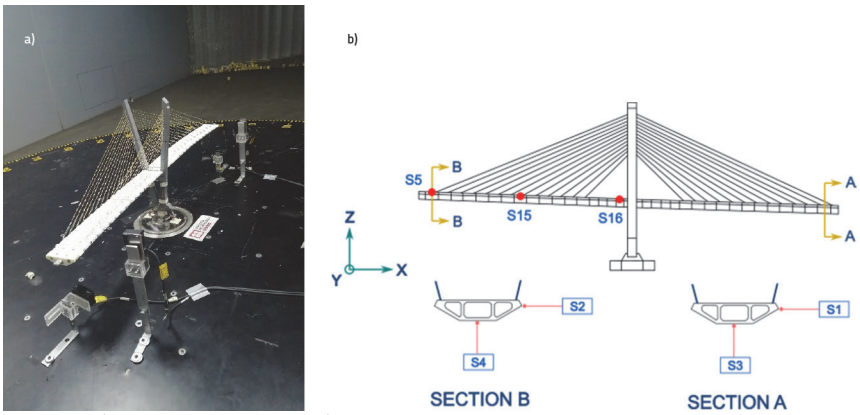

Figure 2 a) Pylon and deck model; b) Sign convention and sensors location

3 Aeroelastic model test procedure

The tests of the full aeroelastic model comprised the recording of time histories at all channels for various responses at each wind speed for a selected range of wind velocities. The mean, root-mean-square (RMS), maximum and minimum values of all measured bridge responses were obtained in a subsequent analysis of the time histories. In the plots of the equivalent prototype response, the peak response is equal to the RMS multiplied by a statistically-based peak factor for random vibration of 3.5 which is considered to be a typical value consistent with turbulent buffeting responses. Thus, the total response is equal to the mean response, plus or minus the peak response. These values were scaled to obtain the bending moments at four sites of the tower, as well as the forces and torque at the base. The definition of flutter is related to the "peak factor", which is defined as the ratio of the largest observed reading during the sample period to the Root Mean Square (RMS). Each of the data points on the response plots result from the measurements of real, stable, limited amplitude motion as opposed to a negative total damping case where the amplitude continues to grow in magnitude for the same wind speed. The peak factor can be used to see whether the motion is in a "locked-in" state of sinusoidal motion or only a random type motion. The total structural response is the result of the mean value plus or minus the g*RMS value [8].

3.1 Smooth flow

A wind tunnel simulation with a "smooth" or very low turbulence (<1%) condition is necessary to identify the potential of vortex shedding induced vibrations and verify that wind speeds associated with flutter instability are sufficiently high [8].

3.1.1 Smooth flow on the isolated pylon

Figure 3 shows an example of the data obtained with the mean and g*RMS values of the recorded strain histories. In this figure we observe the effect of vortex shedding, which occurs at a scaled speed of 40 m/s where the dynamic response is at its highest intensity. Similar plots were obtained for force values F_x, F_y, y F_z at the base of the model. These were obtained directly from the measurements at the load cell, where a peak torque moment was observed on the axis z measurement as well.

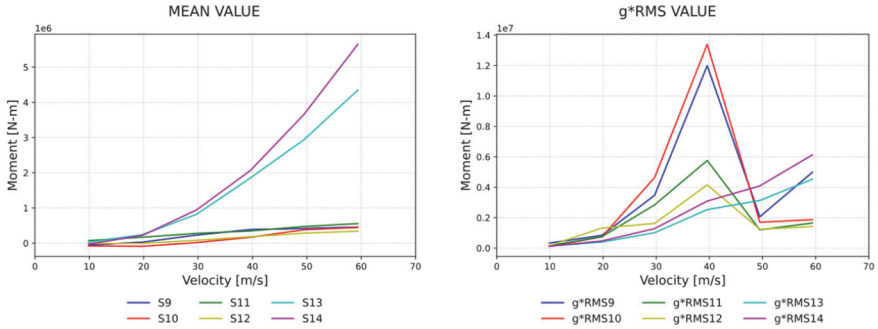

Figure 3 Bending moments at locations S9, S10, S11, S12, S13 and S14, angle of attack 90°, isolated pylon

3.1.2 Dynamic behaviour

An example of a measured (non-scaled) time history of strains obtained with the wind acting on the model with an angle of 90° it's shown in Figure 4; it is worth noting that the S9 and S10 sensors showed the highest responses. The spectral density of the readings suggests that the wind activated a vibration mode higher than 16.03 Hz, which explains the peak RMS value at 40 m/s as shown in Figure 3.

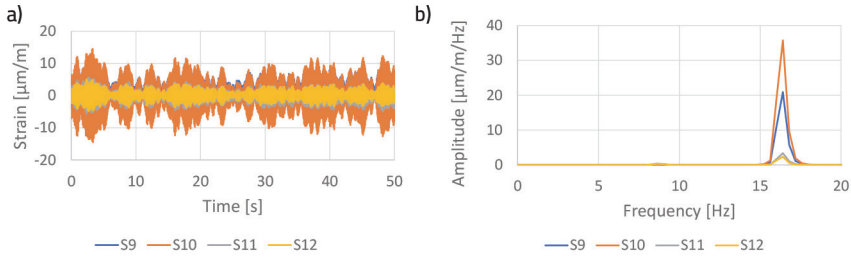

Figure 4 Time histories of strains, locations S9, S10, S11 Y S12; b) Spectral density

As can be seen in Figure 4, the vibration frequency initiated by the wind corresponds to the torsion mode of the tower, which was confirmed by the analysis of pair of signals in the frequency domain as shown in Figure 5, where the simultaneous recordings of the S9 and S10 sensors were compared according to the methodology proposed by Bendat and Piersol [9]. The phase angle function shows a value of -178.91 degrees for the frequency of 16.03 Hz, indicating that there is a relative motion in the opposite direction between the two instrumented locations. The effect of such torsion was also observed in the RMS values of the load cell. It is worth clarifying that this effect does not mean that a vortex shedding is generated, but that this response is attributed to the fact that the upwind arm of tower, where the S9 sensor is located, caused a wake of turbulence which caused the other arm, where the S10 sensor is located, to amplify its vibrations. The second mode of vibration was activated, and this effect can also be seen in the spectral density amplitude where the S10 sensor shows greater amplitude.

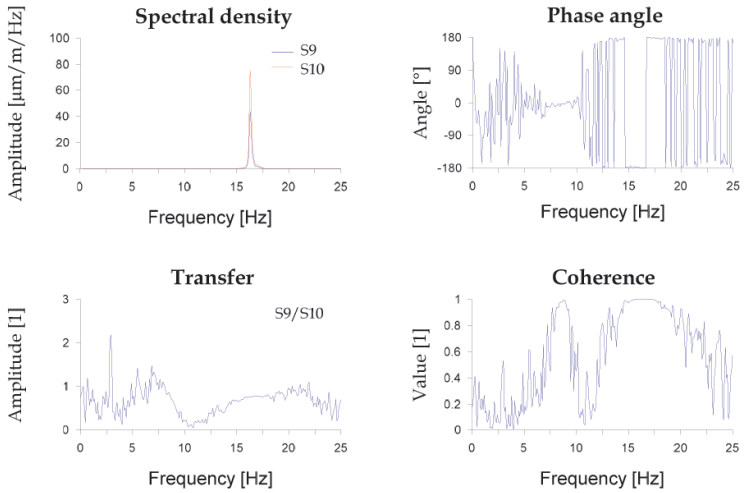

Figure 5 Spectral density, transfer, phase angle and coherence functions of the S9 and S10 sensors records, with 90° angle of attack

3.1.3 Smooth flow on the pylon and deck model

As expected, the incorporation of the superstructure in the scale model increases the bending moments at the pylon foundation, where the bending moments gradually increase as the wind speed increases. Displacements are not significant until they are higher than the design speed, and the largest rotations occur at the 150° angle of attack. Figure 6 shows the response of the pylon with the deck installed.

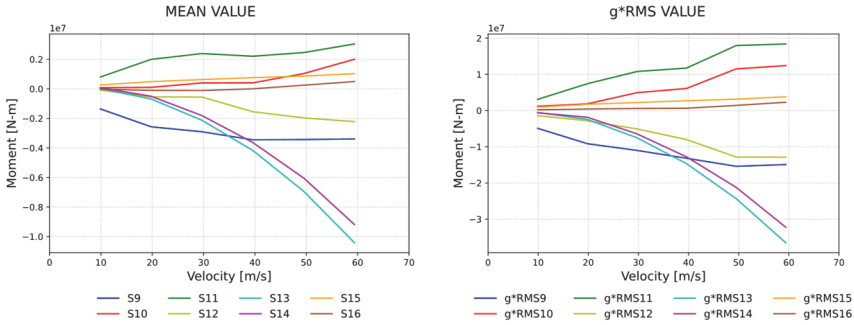

Figure 6 Bending moments at locations S9, S10, S11, S12, S13 S14, S15 and S16, angle of attack 90°, pylon and deck

3.2 Turbulent flow

To carry out the tests in an atmospheric boundary layer, an urban terrain was simulated. Eqn. 1 describes the variation of the mean wind with the height accordingly.

$$\overline{U}(z) = u_{ref}\left(\frac{z}{z_{ref}}\right)^{\alpha} \tag{1}$$

where $\overline{U}(z)$ is the mean velocity corresponding to the z-height, u_{ref} is the reference velocity, z_{ref} is the height corresponding to the reference velocity, and α is the dimensionless exponent of the power law. Figure 7 shows the typical normalized mean wind speed profile of a full-scale urban terrain ($\alpha = 0.28$).

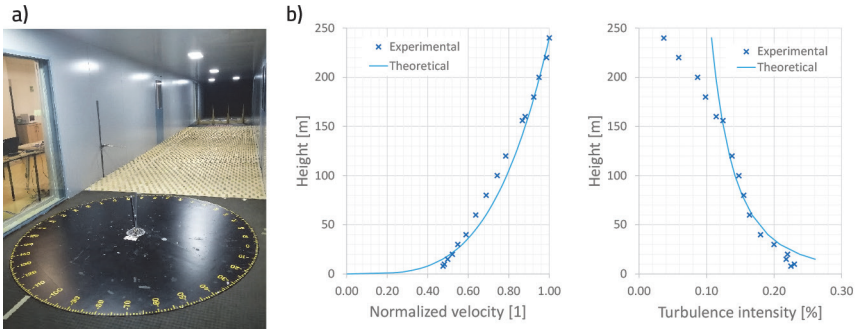

Figure 7 a) Rough elements inside the wind tunnel: b) normailzed experimental mean velocity profile and turbulence intensity

3.2.1 Turbulent flow on the isolated pylon model

Figure 8 shows that the amplitude of the peak observed previously during the smooth flow tests (Figure 3) is still observed but smaller. A greater response in the structure was expected when the flow was turbulent, as in this case.

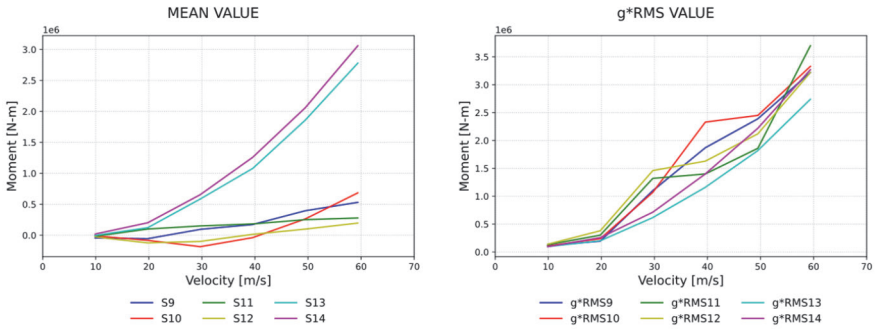

Figure 8 Bending moments, at locations S9, S10, S11, S12, S13 and S14, angle of attack 90°, isolated pylon

3.2.2 Turbulent flow on the pylon and deck model

In turbulent flow, as the wind speed increased, a better trend for the variation of some variables was observed. The magnitudes achieved in both rotations and displacements were very similar to those obtained in the case of smooth flow; for a wind incidence of 150°, the largest rotations of the deck were observed. The structural system remained stable and its response was not significantly amplified at wind speeds below the design speed. Figure 9 shows some results of bending moments.

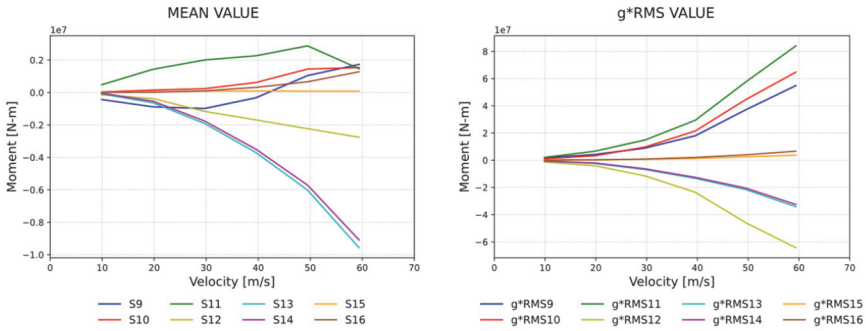

Figure 9 Bending moments at locations S9, S10, S11, S12, S13 S14, S15 and S16, angle of attack 90°, pylon and deck

4 Conclusions

Different ways of placing cables, insulation techniques and sensor arrays were tested, as well as new methodologies for 3D printing of parts in order to install them properly. Tests were performed with low velocities, with and without turbulence, to demonstrate the stability of the measurements and study the dynamic response of the bridge structure.

A velocity that generates torsional vibrations in the Isolated pylon was identified, which corresponds to 40 m/s. This value was compared with the recommended velocity for construction stages (28.88 m/s) and it was observed that this velocity is unlikely to occur at the site because it is higher than the design velocity (36.39 m/s) which corresponds to a return period of 200 years.

The incorporation of the superstructure in the tests revealed that this value of 40 m/s for the 90° angle of wind incidence does not significantly affect the response of the pylon, on the contrary, it shows a better aerodynamic behaviour either in smooth or turbulent wind flow; no major complications are expected in the construction procedure. During the tests, no aeroelastic instabilities like flutter or vortex shedding were observed that could compromise the stability of the bridge.

References

[1] Holmes, J.D.: Prediction of the response of a cable-stayed bridge to turbulence, Proc., 4th Int. Conf. on Wind Effects on Build. and Struct., pp. 187–197, London, 1975.

[2] Cunming, M., Yangzhao, L., Ngai, Y., Qiusheng, L.: Experimental Study of Across-Wind Aerodynamic Behavior of a Bridge Tower, American Society of Civil Engineers, 2018.

[3] Cermak, J.E., et al.: Wind Tunnel Studies of Buildings and Structures Task Committee on Wind Tunnel Testing of Buildings and Structures, American Society of Civil Engineers, 1999.

[4] Micro Measurements-VGP: Stress analysis, https://www.micro-measurements.com/pca/stress-analysis-gages/linear

[5] ATI Industrial Automation: Sensor F/T: Gamma https://www.ati-ia.com/es-MX/products/ft/ft_models.aspx?id = Gamma

[6] Bryan Siepert: MPU6050 6-axis Accelerometer and Gyro, Adafruit learning system, 2019.

[7] KEYENCE: LR-X Series: https://www.keyence.com.mx/products/sensor/photoelectric/lr-x/models/lr-x100c/

[8] King, J.P.C., Kong, L.: A study of wind effects for the El Carrizo Bridge, The Boundary Layer Wind Tunnel Laboratory, The University of Western Ontario, Faculty of Engineering Ontario Canada, October 2012.

[9] Bendat, J.S., Piersol, A.G.: Random data: analysis and measurements procedures, Second edition, Wiley Interscience, New York, 1989.